

# Cerium Oxide-Based Sorbents for Regenerative Hot Reformate Gas Desulfurization

Zheng Wang and Maria Flytzani-Stephanopoulos\*

Department of Chemical and Biological Engineering, Tufts University,  
Medford, Massachusetts 02155

Received December 30, 2004. Revised Manuscript Received May 11, 2005

The activity and stability of lanthanum- or copper-containing cerium oxide sorbents for hot reformat gas desulfurization were investigated in this work. Reformate gas, derived from the catalytic partial oxidation or autothermal reforming of heavy fuels such as JP-8, is rich in hydrogen and CO and may also contain up to 500 ppmv H<sub>2</sub>S. Desulfurization at temperatures in the range of 650–800 °C is required before using the fuel gas in solid oxide fuel cells. In this work, regenerable cerium oxide-based sorbents were used in desulfurization. The sorbents were prepared with high surface area by the urea coprecipitation/gelation method, followed by slow heating and calcination in air at 650 °C for 4 h. Lanthanum doping (up to 50 at. %) was determined to be effective in moderating the surface area loss of cerium oxide (ceria) in H<sub>2</sub>S-free reformat gas at 800 °C. On the other hand, severe sintering occurred when copper was used as an additive, even in amounts as low as 10 at. % copper in ceria. However, the copper-containing ceria had the best sulfidation kinetics among the ceria-based sorbents. Sorbents were evaluated in cyclic sulfidation/regeneration tests at 650 and 800 °C, using a simulated reformat gas mixture in sulfidation, and a 3% O<sub>2</sub>–He gas mixture for regeneration. Using very high space velocities, we determined that sulfidation could be limited to the sorbent surface. The surface sulfur capacity of the sorbents was stable in cyclic sulfidation/regeneration under these conditions.

## Introduction

Fuel cells are currently undergoing rapid development as promising candidates for high-efficiency power generation. Solid oxide fuel cells (SOFCs), operating at high temperatures (>650 °C), are less costly and complex in their processing system, when compared to the low-temperature proton exchange membrane (PEM) fuel cells in which carbon monoxide must be removed from the hydrogen-rich gas mixture, because it poisons the anode catalyst.

Hot reformat gas produced by catalytic partial oxidation (CPOX) or the autothermal reforming of heavy fuels such as JP-8 will have to be desulfurized prior to its use in a SOFC. The desulfurization temperature should match the SOFC temperature of 650–800 °C, to avoid heat-exchanger penalties. Sorbent materials to be used for this application should have favorable sulfidation equilibria, good kinetics, and high structural stability and regenerability. Most single- and mixed-metal oxide sorbents that have been considered in the past for high-temperature desulfurization of coal-derived gas streams are deficient in one or more of the aforementioned properties. Thus, ZnO-based sorbents have low structural stability at high temperatures, because of the reduction to volatile zinc, and zinc migration and agglomeration occurs on the sorbent particle surface.<sup>1–4</sup> Copper oxide-based sorbents have

excellent sulfidation equilibria, if copper is retained in an oxidized state.<sup>5</sup> However, for highly reducing gas compositions and high temperatures, metallic copper is formed, with relatively low sulfidation efficiency.

We have previously reported that mixing CuO with cerium oxide (ceria, CeO<sub>2</sub>) improves the sulfidation efficiency and sulfur capacity of either oxide in uncombined form.<sup>6,7</sup> This cooperative effect is present at both low and high temperatures. At low temperatures (<400 °C), this is explained by the higher extent of surface reduction of cerium oxide to its Ce<sub>2</sub>O<sub>3</sub> form in the presence of copper. The reduced cerium oxide is a superior H<sub>2</sub>S sorbent, whereas CeO<sub>2</sub> is a poor one.<sup>8</sup> At medium high temperatures (up to 500 °C), CeO<sub>2</sub> keeps the copper particles highly dispersed, such that their sulfur capacity is not compromised. Bulk cerium oxide is interesting as a regenerable desulfurization sorbent,

(2) Lew, S.; Sarofim, A. F.; Flytzani-Stephanopoulos, M. *Ind. Eng. Chem. Res.* **1992**, *31*, 1890.

(3) Flytzani-Stephanopoulos, M.; Yu, T. U.; Lew, S. Development and Testing of Desulfurization Sorbents; Topical Report to Texaco, under Subcontract to the U.S. Department of Energy (DOE), No. DE-FC21-87MC23277, 1988.

(4) Mei, J. S.; Gasper-Galvin, L.; Everitt, C. E.; Katta, S. *Proceedings of the Coal-Fired Power Systems '93*; Advances in IGCC and PFBC Review Meeting, DOE/METC-93/6131; June 1993; pp 315–325.

(5) Patrick, V.; Gavalas, G. R.; Flytzani-Stephanopoulos, M.; Jothisurugesan, K. *Ind. Eng. Chem. Res.* **1989**, *28*, 931.

(6) Li, Z.; Flytzani-Stephanopoulos, M. *Ind. Eng. Chem. Res.* **1997**, *36*, 187.

(7) Kobayashi, M.; Flytzani-Stephanopoulos, M. *Ind. Eng. Chem. Res.* **2002**, *41*, 3115.

(8) (a) Kay, D. A. R.; Wilson, W. G. Desulfurization of Fluid Materials, U.S. Patent No. 4,507,149, March 26, 1985. (b) Kay, D. A. R.; Wilson, W. G. Methods of Desulfurizing Gases, U.S. Patent No. 4,826,664, May 2, 1989.

\* Author to whom correspondence should be addressed. E-mail address: mflytzan@tufts.edu.

(1) Lew, S. Ph.D. Thesis, Massachusetts Institute of Technology (MIT), Cambridge, MA, 1990.

because elemental sulfur is produced in high yields in the oxidative regeneration of its sulfides.<sup>9</sup> Doping CeO<sub>2</sub> with rare-earth oxides, such as lanthanum oxide, increases the number of oxygen vacancies and oxygen ion mobility, and it stabilizes CeO<sub>2</sub> against sintering up to 800 °C.<sup>10,11</sup>

In this paper, we report on the high-temperature (650–800 °C) sulfidation activity and structural stability of cerium oxide that has been doped with lanthanum or copper oxide in gas streams simulating reformat-type gases from the CPOX of JP-8 fuel. The suitability of this type of mixed oxide as a regenerable desulfurization sorbent to be used upstream of a SOFC is examined. The effect of high-temperature reduction on the ensuing sorbent properties is systematically evaluated. This is of practical interest for the operation of a fixed-bed of sorbent, which is gradually being sulfided, while it is continuously being reduced by the hydrogen-rich reformat gas. The regenerability of ceria-based sorbents is examined under conditions where sulfidation is limited to the sorbent surface.

## Experimental Procedures

**Sorbent Preparation and Characterization.** Ceria (CeO<sub>2</sub>) samples doped with La<sub>2</sub>O<sub>3</sub> and CuO were prepared using a variation of the urea coprecipitation/gelation method,<sup>12</sup> as adapted previously in our laboratory.<sup>11</sup> For example, to prepare 10 at. % Cu–CeO<sub>2</sub>, 1.8 g copper(II) nitrate (Johnson Matthey Electronics), and 41.1 g ammonium cerium(IV) nitrate (Aldrich) were mixed and dissolved in 600 mL of deionized (DI) water. This gives a Ce/Cu atomic ratio of 9:1. Similarly, to make Ce–30 at. % LaO<sub>x</sub>, 32 g of ammonium cerium(IV) nitrate (Aldrich) and 7.3 g of lanthanum nitrate hydrate (Aldrich) were used to prepare a sample with a Ce/La atomic ratio of 7:3. Excess urea (72 g) was added into the solution under constant stirring and boiling over a hot plate. After the precipitant was produced, DI water was added to 800 mL, and the solution was kept boiling for 8 h. The precipitate was filtered, washed twice, then dried under vacuum at 120 °C for 12 h and crushed to a powder before calcination. Samples were heated to 650 °C in air at a rate of 2 °C/min and then held at the final temperature for 4 h.

The sorbent elemental composition was analyzed by inductively coupled plasma–atomic emission spectrometry (ICP–AES) (Perkin–Elmer, model Plasma 40). The sorbent surface areas were measured by single-point N<sub>2</sub> adsorption/desorption cycles using a Micromeritics model Pulse Chemisorb 2705 flow BET apparatus. X-ray diffraction (XRD) patterns were obtained using a Rigaku model 300 instrument with a rotating anode generator and a monochromatic detector. Cu Kα<sub>1</sub> radiation was used, with a power setting of 60 kV and 300 mA.

**Sorbent Sulfidation Tests.** Sulfidation tests were performed at atmospheric pressure in a packed-bed quartz-tube microreactor (inner diameter of 1.0 cm) to evaluate the sorbent H<sub>2</sub>S removal efficiency and sulfur capacity at 30 ppm H<sub>2</sub>S breakthrough. Particles with a diameter of <53 μm were used in the reactivity tests. Typically, 0.34 g of sorbent was loaded on a quartz frit, which was located at the center of the reactor.

To mimic the conditions of a fixed-bed sorber, where most of the bed is initially exposed to sulfur-free gas, prereduction of the sorbents in H<sub>2</sub>S-free fuel gas at the corresponding sulfidation temperature was performed prior to each sulfidation test. All gas mixtures were of analytical grade (H<sub>2</sub>S (Airgas, 99.5/0.5 He/H<sub>2</sub>S), H<sub>2</sub> (Airgas, 99.999%), helium (Airgas, 99.999%), O<sub>2</sub> (Airgas, 90/10 He/O<sub>2</sub>)). Samples were first heated in helium to the desired sulfidation temperature. A 50% H<sub>2</sub>–10% H<sub>2</sub>O–(balance) He mixture gas was switched in, to prereduce the sorbents for 1 h. The sulfidation gas mixture, which was 0.1% H<sub>2</sub>S–50% H<sub>2</sub>–10% H<sub>2</sub>O–(balance) He, was then introduced. This mixture contains no CO (all is compensated by hydrogen), and an exaggerated amount of H<sub>2</sub>S (0.1%) is used to reduce the testing time. A flow rate of 40 mL/min (NTP) was used in tests conducted at a gas hourly space velocity (SV) of 16 000 h<sup>–1</sup>. H<sub>2</sub>S and SO<sub>2</sub> concentrations in the exit gas were measured on-line, using a Western Research Series 900 UV–Vis analyzer (Ametek). Data from runs at 650 and 800 °C are presented here.

**Kinetic Tests.** Sulfidation kinetic tests were conducted in a Cahn model TG-121 thermogravimetric analyzer (TGA) that was equipped with an electrobalance and a temperature controller. The gas flow rate was controlled by Brooks mass flow controllers and supplied to the TGA at a pressure of 0.10 MPa. The weight change was measured as a function of the time associated with hydrogen sulfide uptake. Isothermal tests were conducted in the temperature range of 600–850 °C.

Because the hot reformat gas contains >20% H<sub>2</sub> and 20% CO, both sulfidation and reduction reactions will happen simultaneously when the sorbent is exposed to it. Sulfidation is typically detected by a sorbent weight increase, whereas reduction leads to a weight decrease. Therefore, to distinguish each step in the TGA, reduction was performed in 50% H<sub>2</sub>–He at 800 °C for 10 min prior to the sulfidation step. In separate tests, we found that 10 min was sufficient time for reduction to occur. A simulated hot reformat gas mixture (0.1% H<sub>2</sub>S, 50% H<sub>2</sub>, and 3% H<sub>2</sub>O, with the balance being helium) was introduced in the TGA after reduction was complete. The total gas flow rate was 500 mL/min. The sample powder was spread on quartz wool that filled a hemispherical quartz pan suspended by a thin quartz hang-down wire. Blank tests were conducted to compensate for the effect of buoyancy and apparent flow rate change. Typically, a load of 4–6 mg sorbent was used. To ensure that the results were obtained in the absence of diffusion limitations, either external (i.e., gas-film diffusion) or internal (i.e., intraparticle diffusion), a small particle size (<53 μm) was used and the flow rate was varied; a flow rate of 500 mL/min was determined to be adequate to eliminate gas–film diffusion limitations.

**Cyclic Sulfidation/Regeneration Tests.** Cyclic sulfidation and regeneration were performed in the quartz-tube flow microreactor. Prior to each sulfidation test, prereduction was conducted with the H<sub>2</sub>S-free gas mixture at the sulfidation temperature for 1 h, then sulfidation was performed at the same temperature at SV = 16 000 or 80 000 h<sup>–1</sup> (NTP), with a gas mixture of 0.1% H<sub>2</sub>S, 50% H<sub>2</sub>, and 10% H<sub>2</sub>O, with the balance being helium. Regeneration was conducted at the same temperature as sulfidation at SV = 80 000 h<sup>–1</sup>. The regeneration gas mixture (3% O<sub>2</sub>–He) was followed by the H<sub>2</sub>S-free reformat gas mixture (50% H<sub>2</sub>–10% H<sub>2</sub>O–He). Each step was performed until the H<sub>2</sub>S and SO<sub>2</sub> exit concentrations were <5 ppm. H<sub>2</sub>S and SO<sub>2</sub> concentrations in the exit gas stream were measured continuously by an ultraviolet–visible (UV–Vis) analyzer (Ametek).

## Results and Discussion

**Characterization of Fresh Sorbents.** Table 1 lists key properties of the fresh (as-prepared) sorbents. All lanthanum- or copper-containing ceria samples have surface areas in the range of 71–100 m<sup>2</sup>/g after calcina-

(9) Zeng, Y.; Zhang, S.; Groves, F. R.; Harrison, D. P. *Chem. Eng. Sci.* **1999**, *54*, 3007.

(10) Trovarelli, A. *Catalysis by Ceria and Related Materials*; Imperial College Press: London, 2002.

(11) Kundakovic, Lj.; Flytzani-Stephanopoulos, M. *Appl. Catal., A* **1998**, *171*, 13.

(12) Amenomiya, Y.; Emesh, A.; Oliver, K.; Pleizer, G. In *Proceedings of the 9th International Congress on Catalysis*; Philips, M., Ternan, M., Eds.; Chemical Institute of Canada: Ottawa, Canada, 1988; p 634.

Table 1. Characterization of Fresh Sorbents<sup>a</sup>

sorbent	BET surface area (m <sup>2</sup> /g)	CeO <sub>2</sub> (111) particle size <sup>b</sup> (nm)	XRD-identified phase(s)	Lattice Parameter $\alpha^c$ (nm)	
				(111)	(220)
CeO <sub>2</sub>	71	9.2	CeO <sub>2</sub>	5.416	5.412
10 at. % Cu–CeO <sub>2</sub>	100	9.6	CeO <sub>2</sub>	5.413	5.403
Ce–30 at. % LaO <sub>x</sub>	85	7.5	CeO <sub>2</sub> , La <sub>2</sub> O <sub>2</sub> CO <sub>3</sub>	5.458	5.442
10 at. % Cu–Ce–30 at. % LaO <sub>x</sub>	81	8.1	CeO <sub>2</sub> , La <sub>2</sub> CuO <sub>4</sub>	5.446	5.433
30 at. % Cu–Ce–30 at. % LaO <sub>x</sub>	79	9.0	CeO <sub>2</sub> , La <sub>2</sub> CuO <sub>4</sub> , CuO	5.428	5.425

<sup>a</sup> Fresh samples were made by urea gelation/coprecipitation and were calcined in air at 650 °C for 4 h. <sup>b</sup> Particle size was calculated by the Scherrer equation. <sup>c</sup> The lattice parameter was calculated from the XRD data, using the formula  $\alpha = \sqrt{h^2 + k^2 + l^2}[\lambda/(2 \sin \theta)]$ , where  $\lambda = 1.54056$  nm.

Table 2. Effect of Gas and Heat Treatment on Sorbent Surface Area

sorbent	Specific Surface Area after Treatment (m <sup>2</sup> /g)							
	In Air		In 50% H <sub>2</sub> –He <sup>a</sup>		In 50% H <sub>2</sub> –10% H <sub>2</sub> O–He <sup>a</sup>		Used Sample <sup>a,b</sup>	
	650 °C, 4 h	800 °C, 10 h	800 °C, 10 min	800 °C, 2 h	650 °C, 1 h	800 °C, 1 h	650 °C	800 °C
CeO <sub>2</sub>	71	14.4	19.5	16.2	73.1	25.1	55.3	17.8
Ce–10 at. % LaO <sub>x</sub>	100	56.5	24.8	19.7	73.2	32.3	N/A	N/A
Ce–30 at. % LaO <sub>x</sub>	85	45.5	25	21.3	61	28.3	51.1	25.2
Ce–50 at. % LaO <sub>x</sub>	87.2	39	22.7	18.5	59.7	25.9	N/A	N/A
Ce–70 at. % LaO <sub>x</sub>	85.3	21.4	14.7	10.4	38.2	13.8	N/A	N/A
La <sub>2</sub> O <sub>3</sub>	5	2	3	~1	3.4	1.4	N/A	N/A
10 at. % Cu–CeO <sub>2</sub>	100	<1	<1	<1	56.5	<1	42.6	<1

<sup>a</sup> Sorbents were first calcined in air at 650 °C for 4 h; the surface area of each material after calcination is shown in the first column.

<sup>b</sup> The surface area was measured after sorbent was used in five cycles of sulfidation/regeneration tests at a sulfidation space velocity of SV = 80 000 h<sup>−1</sup> and regeneration space velocity of SV = 80 000 h<sup>−1</sup>.

tion at 650 °C in air for 4 h. The crystallite size of CeO<sub>2</sub> in each sample was calculated using the Scherrer equation, based on the corresponding XRD pattern. As shown in Table 1, the average particle size of as-prepared CeO<sub>2</sub> is 9.2 nm. Lanthanum doping at a level of 30 at. % reduces the particle size to 7.5 nm. A similar effect of lanthanum was observed when copper was also present in the sorbent. CeO<sub>2</sub> crystal growth to 10.2 nm was observed in 10 at. % Cu–CeO<sub>2</sub>, whereas, when both copper and lanthanum were present, a smaller CeO<sub>2</sub> particle size was observed in 10 at. % Cu–Ce–30 at. % LaO<sub>x</sub> (8.1 nm), even up to a copper doping level of 30 at. % (9.0 nm), compared to that of 10 at. % Cu–CeO<sub>2</sub>.

As identified by XRD, all sorbents have the distinct fluorite oxide-type structure of CeO<sub>2</sub>. No copper oxide phase was detected in 10 at. % Cu–CeO<sub>2</sub>. This indicates that copper oxide exists in a highly dispersed form, in agreement with a previous report.<sup>7</sup> Most lanthanum oxide was in solid solution with ceria, as indicated by the lattice constant expansion (see Table 1) of the latter. In addition, the presence of La<sub>2</sub>O<sub>2</sub>CO<sub>3</sub> was observed in Ce–30 at. % LaO<sub>x</sub>, whereas La<sub>2</sub>CuO<sub>4</sub> was identified in the ternary oxide sorbent 10 at. % Cu–Ce–30 at. % LaO<sub>x</sub>. Copper oxide was found only in samples with high copper content (>20 at. %).

The surface areas of a series of ceria samples with different lanthanum contents are shown in Table 2. After calcination at 650 °C for 4 h in air, the surface area of ceria and lanthanum doped-ceria with a lanthanum content of up to 70 at. % is >80 m<sup>2</sup>/g, whereas that of bulk La<sub>2</sub>O<sub>3</sub> is only 5 m<sup>2</sup>/g. Apparently, ceria can disperse lanthana quite well, even at contents exceeding the amount of lanthana that can be in solid solution with ceria. According to a recent report,<sup>13</sup> the maximum

amount of lanthana that can be in solid solution with ceria is 60 at. %.

As expected, materials calcined at 800 °C for 10 h in air had lower surface areas than the samples that were calcined at 650 °C. Ce–10 at. % LaO<sub>x</sub> had the highest surface area (~55 m<sup>2</sup>/g). As the lanthanum content increased, the surface area of the sorbent decreased. Ceria that was doped with 70 at. % lanthanum still has a surface area of 21 m<sup>2</sup>/g, whereas pure ceria has a surface area of 15 m<sup>2</sup>/g; i.e., it has suffered over 80% surface area loss, compared to the sample that was calcined at 650 °C. Consistently, therefore, under all conditions, lanthanum doping improves the stability of ceria against crystal growth and sintering, as was also reported earlier.<sup>11</sup>

The effect of copper addition in ceria is different. As shown in Table 2, after calcination at 650 °C for 4 h in air, the surface area of 10 at. % Cu–CeO<sub>2</sub> is 30% higher than that of pure CeO<sub>2</sub>. After calcination at 800 °C for 10 h in air, however, the surface area of 10 at. % Cu–CeO<sub>2</sub> decreases dramatically to 1 m<sup>2</sup>/g, which is a much smaller value than that of pure ceria (15 m<sup>2</sup>/g). This shows that copper enhances the sintering of ceria at this temperature. XRD patterns were collected on differently treated 10 at. % Cu–CeO<sub>2</sub> to confirm this sintering effect. For the material that was calcined at 650 °C, as shown in Figure 1, no copper oxide reflections were detected by XRD. This indicates that copper oxide exists in a highly dispersed form in ceria. Data analysis of the XRD pattern shows that the average crystallite size of this 10-at. %-copper-containing cerium oxide was 9.6 nm. However, large CuO particles (>100 nm) were observed after heat treatment of the sorbents in air at 800 °C for 10 h. Treatment in 50% H<sub>2</sub>/He for 10 min at 800 °C also had a dramatic effect on surface area loss (see Table 2), and large metallic copper particles (80 nm) were identified by XRD (see Figure 1, inset). The



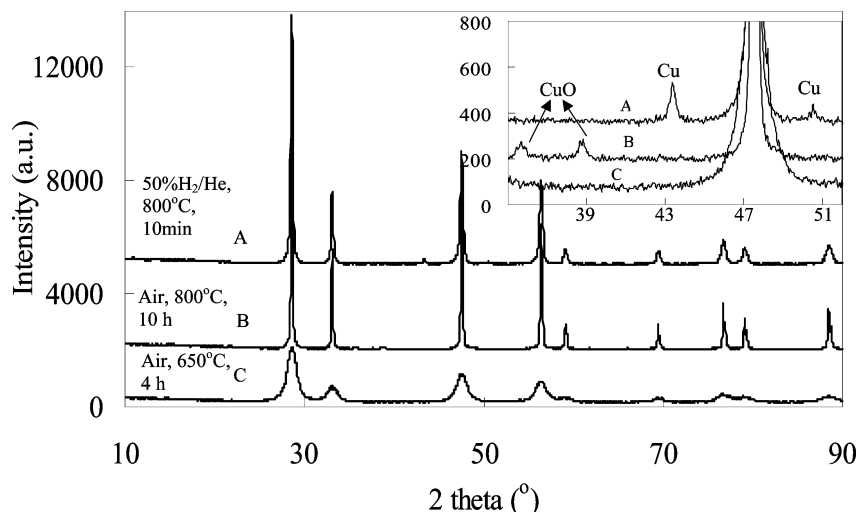


**Figure 1.** X-ray diffractograms of 10 at. % Cu–CeO<sub>2</sub> as-prepared (calcined at 650 °C for 4 h in air) and after further heating in air or H<sub>2</sub> gas at 800 °C.

corresponding cerium oxide particle sizes were 94.8 and 48.5 nm, respectively, after these two heat treatments.

**Effect of Reduction on Sorbent Properties.** In a typical fixed-bed sulfidation process, initially sulfidation of the top layer of the sorbent occurs while the remainder of the sorbent is being exposed to H<sub>2</sub>S-free reformat gas. Therefore, it is necessary to examine potential structural effects of this reduction process on the sorbent properties. For practical application, the prereduced sorbent structure, rather than the fresh one, is important in rank ordering the activity/regenerability of various sorbent compositions. The surface areas of selected sorbents after exposure to the H<sub>2</sub>S-free 50% H<sub>2</sub>–10% H<sub>2</sub>O–He gas mixture at different temperatures are listed in Table 2. Prior to the reduction test, each sorbent had been calcined at 650 °C for 4 h in air. The corresponding initial surface areas are also shown in Table 2 (in the first column). Compared to the as-prepared sorbents, after prereduction at 650 °C, the surface areas of all sorbents decreased appreciably. When the reduction temperature increased to 800 °C, the loss of surface area was higher for all sorbent compositions. Clearly, the most dramatic surface area loss is suffered by the copper-containing ceria samples at 800 °C. However, these materials retain adequate surface area after reduction at 650 °C.

**Thermodynamic Considerations.** Figure 2 shows the calculated sulfidation equilibria of CeO<sub>2</sub>, Ce<sub>2</sub>O<sub>3</sub>, La<sub>2</sub>O<sub>3</sub>, and copper in a gas mixture of 50% H<sub>2</sub>–10% H<sub>2</sub>O–He.<sup>14,15</sup> This gas simulates the reformat gas from CPOX of JP-8 fuel, with all CO compensated by H<sub>2</sub>.<sup>16</sup>

Under these highly reducing conditions, CuO<sup>14,15</sup> is readily reduced to metallic copper, and the sulfidation product of copper is cuprous sulfide (Cu<sub>2</sub>S).<sup>17</sup> According to the Ce–O–S system phase diagram established by

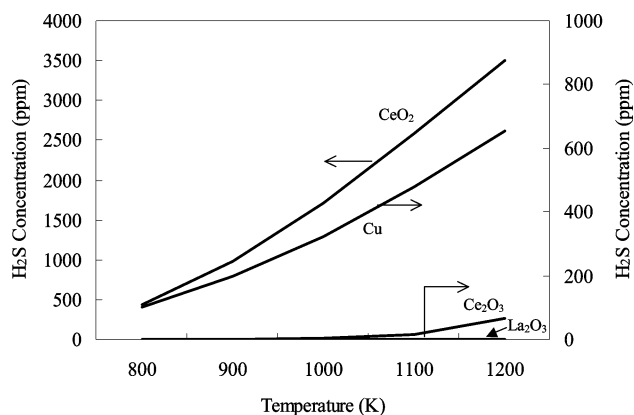


**Figure 2.** Sulfidation equilibria in a gas containing 50% H<sub>2</sub>–10% H<sub>2</sub>O–(balance) He.<sup>14,15</sup>

Kay and Wilson,<sup>18</sup> at the oxygen potential of 10<sup>–20</sup> atm and at 800 °C, the sulfidation product of cerium oxide is cerium oxysulfide, Ce<sub>2</sub>O<sub>2</sub>S. Similarly, La<sub>2</sub>O<sub>2</sub>S<sup>19</sup> is the sulfidation product of La<sub>2</sub>O<sub>3</sub>. The corresponding reactions are shown below:

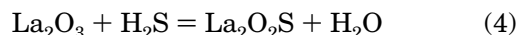
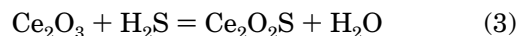
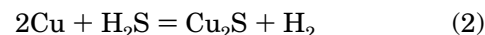
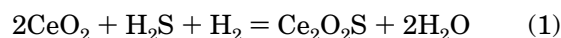


Figure 2 shows that both La<sub>2</sub>O<sub>3</sub> and reduced ceria (Ce<sub>2</sub>O<sub>3</sub>) are superior H<sub>2</sub>S sorbents that keep the H<sub>2</sub>S content at <30 ppm, even up to 1200 K in the gas mixture of interest. On the other hand, fully oxidized CeO<sub>2</sub> has a very low sulfidation equilibrium constant, much lower than metallic copper. The sulfidation equilibrium constant of metallic copper is several orders of magnitude lower than that of CuO or Cu<sub>2</sub>O.<sup>14,15</sup> As shown in Figure 2, the H<sub>2</sub>S equilibrium concentrations are >100 ppm over metallic copper in the temperature

(14) Barin, I.; Sauert, F.; Schultze-Rhonhof, E.; Sheng, W. S. *Thermochemical Data of Pure Substances Parts I and II*; VCH: Weinheim, Germany, 1993.

(15) (a) Barin, I.; Knacke, O. *Thermochemical Properties of Inorganic Substances*; Springer-Verlag: New York, 1973. (b) Barin, I.; Knacke, O.; Kubaschewski, O. *Thermochemical Properties of Inorganic Substances, Supplement*; Springer-Verlag: New York, 1977.

(16) Huss, S. Honeywell Corporation, private communication.

(17) Swisher, J. H.; Schwerdtfeger, K. *J. Mater. Eng. Perform.* **1992**, 1, 399.

(18) Kay, D. A. R.; Wilson, W. G.; Jalan, V. *J. Alloy Compd.* **1993**, 193, 11.

(19) Rajagopalan, V.; Amiridis, M. D. *Ind. Eng. Chem. Res.* **1999**, 38, 3886–3891.

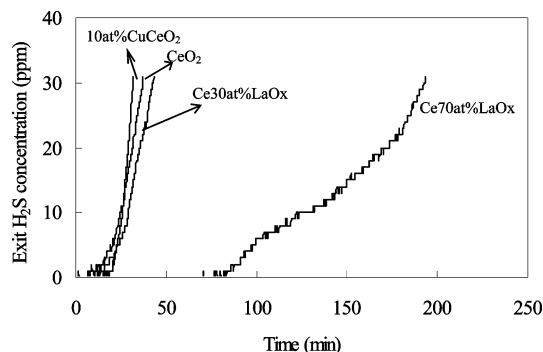


**Figure 3.**  $\text{H}_2\text{S}$  breakthrough curves in first sulfidation cycle of prereduced sorbents. Prereduction:  $T = 650\text{ }^\circ\text{C}$ , 50%  $\text{H}_2$ –10%  $\text{H}_2\text{O}$ –He, space velocity of  $\text{SV} = 80\,000\text{ h}^{-1}$ . Sulfidation:  $T = 650\text{ }^\circ\text{C}$ , 0.1%  $\text{H}_2\text{S}$ –50%  $\text{H}_2$ –10%  $\text{H}_2\text{O}$ –He,  $\text{SV} = 16\,000\text{ h}^{-1}$ .

range of 800–1200 K. These levels exceed the tolerance of current SOFC anodes. Based on Figure 2,  $\text{La}_2\text{O}_3$  and  $\text{Ce}_2\text{O}_3$ , but not  $\text{CeO}_2$ , will be the desulfurization agents in this reformat-type gas mixture. Copper will participate, but only when the  $\text{H}_2\text{S}$  level in the gas exceeds the equilibrium level.

**Sulfidation Tests in the Microreactor.** Figure 3 shows the  $\text{H}_2\text{S}$  breakthrough profile from the first sulfidation of prereduced sorbents to an exit value of 30 ppm  $\text{H}_2\text{S}$ . The corresponding sulfur loadings calculated for the conditions of Figure 3 ( $T = 650\text{ }^\circ\text{C}$ ,  $\text{SV} = 16\,000/\text{h}$ ), as well as for other sulfidation test conditions (i.e., for  $T = 650\text{ }^\circ\text{C}$ ,  $\text{SV} = 80\,000/\text{h}$ ;  $T = 800\text{ }^\circ\text{C}$ ,  $\text{SV} = 16\,000/\text{h}$ ; and  $T = 800\text{ }^\circ\text{C}$ ,  $\text{SV} = 80\,000/\text{h}$ ) are shown in Table 3. Among the selected sorbents, Ce–70 at. %  $\text{LaO}_x$  has the highest sulfidation capacity under all conditions. This is attributed to the participation of lanthanum oxide in sulfidation. One advantage of lanthanum oxide over ceria is that, at all temperatures and reducing gas compositions, it is in the proper oxidation form ( $\text{La}_2\text{O}_3$ ), with a high affinity for  $\text{H}_2\text{S}$  (see Figure 2). On the other hand, only a fraction of  $\text{CeO}_2$  is reduced to  $\text{Ce}_2\text{O}_3$  in a gas containing 50%  $\text{H}_2$ –10%  $\text{H}_2\text{O}$ , even at  $800\text{ }^\circ\text{C}$ . The upper limit can be estimated from thermodynamics<sup>20</sup> to be 33%  $\text{Ce}_2\text{O}_3$  (corresponding to an average formula of  $\text{CeO}_{1.83}$ ). The experimental results reported here do not change if half of the  $\text{H}_2$  in the fuel gas is replaced by  $\text{CO}$ .<sup>21</sup>

Although the sulfur loading is reported in terms of milligrams of sulfur per gram of sorbent, the sorbent surface area is of key importance, in regard to determining the surface sulfur loading. In fact, under certain operating conditions, e.g., when using high space velocities, the sorbent sulfidation will be limited to the surface only.<sup>22</sup> There is a major effect of prereduction on the sorbent surface area, as discussed previously (Table 2). For the tests shown in Table 3, we estimate that sulfidation is limited largely to the surface of each sorbent at the high sulfidation space velocities used in these tests. Thus, the surface area and the extent of surface reduction of  $\text{CeO}_2$  to  $\text{Ce}_2\text{O}_3$  will both determine the surface sulfur capacity of each sorbent. As can be

seen in Table 3, although the sulfidation capacity at  $800\text{ }^\circ\text{C}$  is less than that at  $650\text{ }^\circ\text{C}$ , the value does not scale with the surface area. One limiting factor is the amount (percentage) of  $\text{Ce}_2\text{O}_3$  that is available. Thus, the lower extent of  $\text{CeO}_2$  reduction at  $650\text{ }^\circ\text{C}$  must limit the sulfur loading at this temperature. Moreover, it is possible that, at both  $650$  and  $800\text{ }^\circ\text{C}$ , some bulk sulfidation occurs at a sulfidation space velocity of  $\text{SV} = 16\,000\text{ h}^{-1}$ , whereas at  $\text{SV} = 80\,000\text{ h}^{-1}$ , most sulfidation reaction is limited to the sorbent surface.

Using the sorbent surface area measured after prereduction at each temperature (see Table 2), the surface sulfur capacities of two sorbents—undoped ceria and 30% lanthanum-doped ceria—were estimated. The surface composition of the Ce–30 at. %  $\text{LaO}_x$  used in this calculation was determined by X-ray photoelectron spectroscopy (XPS)<sup>21</sup> and was observed to be similar to its bulk composition as determined by ICP,<sup>21</sup> even after prereduction. Several assumptions were made to calculate the surface sulfur capacity for monolayer adsorption of  $\text{H}_2\text{S}$ : namely, the sorbent surfaces are dominated by the ceria (111) face, which was reported as the most stable face in ceria, even after prereduction;<sup>10</sup> only reduced ceria ( $\text{Ce}_2\text{O}_3$ ) was assumed to participate in sulfidation, and partially reduced ceria ( $\text{CeO}_{1.83}$ ) was used in the calculation for both  $650$  and  $800\text{ }^\circ\text{C}$ .<sup>14,15,20</sup> an upper sulfur loading limit was calculated assuming that each Ce or La atom binds one S atom, whereas a lower limit was calculated assuming that sulfur binds to two Ce or La atoms. The calculated results for  $650$  and  $800\text{ }^\circ\text{C}$  are, respectively, 2.2–4.4 and 0.8–1.6 mg S/g sorbent for  $\text{CeO}_2$ , and 3.5–7.0 and 1.5–3.0 mg S/g sorbent for Ce–30%  $\text{LaO}_x$ . Compared to the experimental values of Table 3, the calculated surface sulfur loadings are similar. This is particularly true for the runs that have been performed at the high space velocity of  $\text{SV} = 80\,000\text{ h}^{-1}$ .

A few experiments were conducted until breakthrough of  $\text{H}_2\text{S}$  at the inlet gas concentration of 0.1% occurred. As shown in Table 4, in all deeply sulfided sorbents, some lanthana was present as oxysulfide ( $\text{La}_2\text{O}_2\text{S}$ ), whereas the remaining lanthana was in oxide solid solution with ceria. These results show that lanthana participates in sulfidation.<sup>19</sup> Besides  $\text{La}_2\text{O}_2\text{S}$ , which is the only sulfide phase observed in both used Ce–30 at. %  $\text{LaO}_x$  and 10 at. % Cu–Ce–30 at. %  $\text{LaO}_x$  sorbents,  $\text{Ce}_2\text{S}_3$  and  $\text{Cu}_2\text{S}$  were also identified in the used 30 at. % Cu–Ce–30 at. %  $\text{LaO}_x$  (see Table 4). The absence of  $\text{Ce}_2\text{O}_2\text{S}$  from the XRD analysis of the samples shown in Table 4 is understood, in view of the reported oxidation of this compound in air at room temperature to the form  $\text{Ce}_2\text{O}_{2.5}\text{S}$ .<sup>23</sup> The BET surface areas of sorbents used in deep sulfidation are also shown in Table 4. After deep sulfidation, all surface areas were considerably lower than those of the as-prepared sorbents (see Table 1), and appreciable ceria crystal growth happened in all three samples (Ce–30 at. %  $\text{LaO}_x$ , 10 at. % Cu–Ce–30 at. %  $\text{LaO}_x$ , and 30 at. % Cu–Ce–30 at. %  $\text{LaO}_x$ ). These effects are suppressed in cyclic operation when sulfidation is limited to the surface of the sorbent. This can be seen by comparing the BET surface area of Ce–30%  $\text{LaO}_x$  after deep sulfidation at

(20) Ferrizz, R. M.; Gorte, R. J.; Vohs, J. M. *Appl. Catal., B* **2003**, 43, 273.

(21) Wang, Z. Ph.D. Thesis work, Tufts University, Medford, MA, in progress.

(22) Flytzani-Stephanopoulos, M.; Wang, Z.; Sakbodin, M. Patent Application No. 60/645,133, November 8, 2004.

(23) Sourisseau, C.; Cavagnat, R.; Mauricot, R.; Boucher, F.; Evain, M. *J. Raman Spectrosc.* **1998**, 28 (12), 965–971.

**Table 3. Sulfur Loading at 30 ppm H<sub>2</sub>S Breakthrough on Prerduced Sorbents<sup>a</sup>**

Operating Conditions		Sulfur Loading (mg S/g sorbent)			
temp (°C)	sulfidation space velocity (h <sup>-1</sup> )	CeO <sub>2</sub>	10 at. % Cu–CeO <sub>2</sub>	Ce–30 at. % LaO <sub>x</sub>	Ce–70 at. % LaO <sub>x</sub>
650	16 000	6.0	4.1	7.2	32.5
650	80 000	3.0	3.5	3.9	19.1
800	16 000	3.7	1.5	5.8	28.8
800	80 000	1.8	1.6	2.7	20.1

<sup>a</sup> Data are for a first-time sulfidation of prerduced sorbents at 650 or 800 °C in 50% H<sub>2</sub>–10% H<sub>2</sub>O–He at a space velocity of SV = 80 000 h<sup>-1</sup>. Sulfidation gas composition: 0.1% H<sub>2</sub>S–50% H<sub>2</sub>–10% H<sub>2</sub>O–He.

**Table 4. Characterization of Sorbents Used in Deep Sulfidation<sup>a</sup>**

sorbent	BET surface area (m <sup>2</sup> /g)	CeO <sub>2</sub> (111) particle size <sup>b</sup> (nm)	XRD-identified phases
Ce–30 at. % LaO <sub>x</sub>	37.7	8.9	CeO <sub>2</sub> , La <sub>2</sub> O <sub>3</sub> S
10 at. % Cu–Ce–30 at. % LaO <sub>x</sub>	18.3	18.5	CeO <sub>2</sub> , La <sub>2</sub> O <sub>3</sub> S
30 at. % Cu–Ce–30 at. % LaO <sub>x</sub>	21.3	14.7	CeO <sub>2</sub> , La <sub>2</sub> O <sub>3</sub> S, Ce <sub>2</sub> S <sub>3</sub> , Cu <sub>2</sub> S

<sup>a</sup> Used samples were sulfided at 650 °C in 0.1% H<sub>2</sub>S–50% H<sub>2</sub>–10% H<sub>2</sub>O–(balance) He gas mixture for over 4 h, at a space velocity of SV = 16 000 h<sup>-1</sup>. <sup>b</sup> Particle size was calculated from the XRD data, using the Scherrer equation.

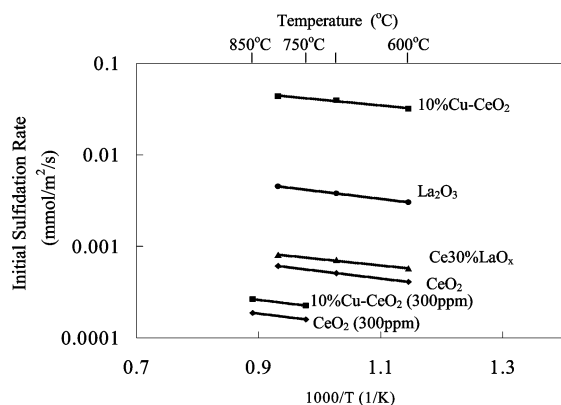


**Figure 4.** Arrhenius-type plot of the initial sulfidation rate of prerduced CeO<sub>2</sub>-based sorbents. Prerduction: 50% H<sub>2</sub>–He at 800 °C. Sulfidation: (0.1% or 0.03%) H<sub>2</sub>S–50% H<sub>2</sub>–10% H<sub>2</sub>O–He, 500 mL/min.

650 °C (see Table 4) and after five cycles of sulfidation/regeneration, also at 650 °C (see Table 2).

**Initial Sulfidation Rates of Ceria-Based Sorbents.** The initial sulfidation rates of prerduced sorbents were measured in the TGA at a flow rate of 500 mL/min, which was sufficiently high for the measured rate to be unaffected by mass-transfer limitations. The collected rate measurements are shown in Figure 4 in an Arrhenius-type plot. The reaction rates are expressed in units of mmol H<sub>2</sub>S adsorbed m<sup>-2</sup> sorbent s<sup>-1</sup>. The sorbent surface area after prerduction at 800 °C was used to normalize the initial sulfidation rate. The sorbent 10 at. % Cu–CeO<sub>2</sub> had the highest sulfidation rate (several orders of magnitude higher than the sulfidation rate of prerduced pure ceria). Lanthanum doping at a level of 30 at. % also improves the sulfidation rate of ceria but was well below that of the 10 at. % Cu–CeO<sub>2</sub> sample. The calculated apparent activation energies of sulfidation are 15 ± 2 kJ/mol for all sorbents, which is similar to the values reported in an earlier paper.<sup>7</sup>

To distinguish the contributions of ceria and copper to the sulfidation rate, we varied the H<sub>2</sub>S concentration so that the sulfidation conditions crossed the phase boundary between metallic copper and copper sulfide. Thus, through the use of a sulfidation gas containing only 300 ppm of H<sub>2</sub>S, at temperatures of 750 and 850 °C, no copper sulfidation should occur, according

to thermodynamic calculations (see Figure 2). As can be seen in Figure 4, the initial sulfidation rate of 10 at. % Cu–CeO<sub>2</sub> is now similar to that of copper-free CeO<sub>2</sub>. Thus, as expected, copper is not being sulfided, and the measured rate is that of reduced cerium oxide. This sulfidation rate is ~3 times less than that of CeO<sub>2</sub> measured at the higher H<sub>2</sub>S concentration (0.1%). Assuming a first-order sulfidation reaction rate, this difference is easy to explain. These tests have thus established that metallic copper has faster sulfidation kinetics than reduced cerium oxide, whereas the sulfidation reactions of both sorbents have similar apparent activation energies. The utility of copper as an additive to ceria is for reformat gas streams that contain more than a few hundred ppmv of H<sub>2</sub>S, such as coal-gasifier exit gas streams.<sup>6,7</sup>

**Cyclic Sulfidation Regeneration Tests.** The cyclic sulfidation/regeneration performance of 10 at. % Cu–CeO<sub>2</sub> and Ce–70 at. % LaO<sub>x</sub> sorbents was examined at 650 and 800 °C. Prerduction in a 50% H<sub>2</sub>–10% H<sub>2</sub>O–He gas mixture was conducted at the corresponding sulfidation test temperature for 1 h. A gas mixture with 3% O<sub>2</sub>/He was used for regeneration, followed by reduction in the 50% H<sub>2</sub>–10% H<sub>2</sub>O–He gas mixture. The sulfur loadings at 30 ppm H<sub>2</sub>S breakthrough are shown in Figure 5 for Ce–70 at. % LaO<sub>x</sub>. The sulfur capacities for the first cycle under both sulfidation temperatures (650 and 800 °C) are similar to each other and are the highest (~30 mg S/g sorbent) among all cycles. A decrease in sulfur loading occurred with cycling, reaching a stable level of 3–4 mg S/g sorbent after the third cycle. There is no significant temperature effect on the stabilized sulfur loading of Ce–70 at. % LaO<sub>x</sub> at the two different temperatures. This can be explained by the presence of a large amount of lanthanum oxide in this sorbent. As discussed previously, prerduction does not change the oxidation state of lanthanum oxide; thus, the temperature effect on the extent of cerium oxide reduction here is not as important as in the cerium oxide-rich sorbents. Surface sulfidation only is displayed after the first two cycles. This is due to the high space velocity used in the tests. However, the much higher sulfur loading in the first cycle indicates irreversible bulk absorption by the lanthana portion of the sorbent. Because of the very high space velocity used in regeneration (80 000 h<sup>-1</sup>), the absorbed amount of sulfur in



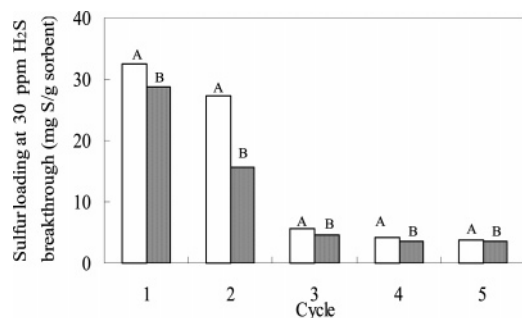
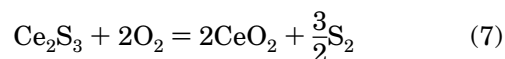
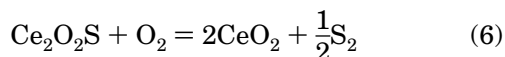


**Figure 5.** Sulfur capacity of Ce-70% LaO<sub>x</sub> at 30 ppm H<sub>2</sub>S breakthrough in cyclic sulfidation/regeneration tests. Conditions for the results presented in panel A were as follows: prereduction: 650 °C, SV = 80 000 h<sup>-1</sup>; sulfidation: 650 °C, SV = 16 000 h<sup>-1</sup>; regeneration: 650 °C, SV = 80 000 h<sup>-1</sup>. Conditions for results presented in panel B were as follows: prereduction: 800 °C, SV = 80 000 h<sup>-1</sup>; sulfidation: 800 °C, SV = 16 000 h<sup>-1</sup>; regeneration: 800 °C, SV = 80 000 h<sup>-1</sup>. For both panels, the prereduction gas composition was 50% H<sub>2</sub>-10% H<sub>2</sub>O-He, the sulfidation gas composition is 0.1% H<sub>2</sub>S-50% H<sub>2</sub>-10% H<sub>2</sub>O-He, and the regeneration gas composition was 3% O<sub>2</sub>-He.

the first 1–2 cycles is retained in the bulk, whereas the stabilized amount of sulfur loaded in subsequent cycles is attributed to surface sulfidation only.

The type and amount of sulfur species eluted during the regeneration and reduction steps are shown in Table 5. Only the stabilized results, which were obtained after two cycles, are shown. Similar regeneration off-gas distributions were obtained at both temperatures that were examined when the sulfidation space velocity was SV = 16 000 h<sup>-1</sup>. At 650 °C, for example, ~52% of the total adsorbed sulfur was eluted in regeneration, in the form of H<sub>2</sub>S and SO<sub>2</sub> at a ratio of 10:1. Another ~26% was eluted in the following reduction step, mostly as H<sub>2</sub>S, with only ~2% in the form of SO<sub>2</sub>. The sulfur species eluted during the reduction step indicate sulfate formation during the regeneration step. This is thought to be a result of reaction of the SO<sub>2</sub> eluted during regeneration with some of the oxide sorbent. Also, the total sulfur balance is <100%, with ~22% of the sulfur being unaccounted for. Equilibrium calculations show that elemental sulfur can be formed during oxidative regeneration of cerium sulfides:<sup>9,14,15</sup>



Elemental sulfur is gaseous and undetectable in the experimental setup that has been used here.

Figure 6 shows the cyclic sulfidation capacity of 10 at. % Cu-CeO<sub>2</sub> at 30 ppmv H<sub>2</sub>S breakthrough. We see that this sorbent has good regenerability already from the first cycle at both temperatures (650 and 800 °C). At the space velocity of SV = 16 000 h<sup>-1</sup>, the sulfur capacity at 650 °C (~5 mg S/g sorbent) is higher than that at 800 °C (1–1.3 mg S/g sorbent). This can be attributed to two reasons. First, reversible sulfidation of the copper component of this sorbent occurs at 650 °C. However, the contribution of copper is lost at

800 °C, because of the severe sintering of the copper and ceria particles (see Table 2) and to the lower affinity of copper for H<sub>2</sub>S at 800 °C (see Figure 2). The second reason is that more-extensive bulk sulfidation occurs at 650 °C. This was further probed by performing the experiments at 650 °C under higher sulfidation space velocity (SV = 80 000 h<sup>-1</sup>). As shown in Figure 6, lower sulfur capacity was then measured.

Table 5 lists the sulfur species eluted during the regeneration and reduction steps from 10% Cu-CeO<sub>2</sub> after it was sulfided at a sulfidation of SV = 16 000 h<sup>-1</sup>. At 650 °C, ~51% of the adsorbed sulfur was eluted as H<sub>2</sub>S and SO<sub>2</sub> with a ratio of 1:1 in 3% O<sub>2</sub>-He. Another 38% of the sulfur was eluted in the following reduction step, with 15% of total adsorbed amount in the form of SO<sub>2</sub>. Again, these results indicate sulfate formation during the regeneration step. The extent of sulfate formation is higher than that for the Ce-70% LaO<sub>x</sub> sorbent, as also shown in Table 5. Also, the amount (percentage) of H<sub>2</sub>S adsorbed that was eluted as elemental sulfur is approximately one-half of that of the Ce-70% LaO<sub>x</sub> sorbent. We attribute these effects to the presence of copper in this sorbent. Copper is known to enhance the sulfation of cerium oxide.<sup>24</sup> Also, copper sulfate can be stable at 650 °C.<sup>24,25</sup> Finally, copper sulfide cannot produce elemental sulfur in oxidative regeneration.<sup>14,15</sup> Regeneration at 800 °C suppressed the formation of sulfates. Compared to the 650 °C case, much more H<sub>2</sub>S was eluted in the 3% O<sub>2</sub>/He regeneration step (57% vs 25%), whereas less SO<sub>2</sub> was produced (14% vs 26%). During the reduction step, very little SO<sub>2</sub> (3%) was measured. The data are now similar to the copper-free sorbents that are shown in Table 5.

The effect of higher sulfidation space velocity (SV = 80 000 h<sup>-1</sup>) on the sorbent sulfur capacity was investigated at 800 °C. Results are shown in Figure 7 for three different sorbents, including undoped ceria. For all sorbents, increasing the sulfidation space velocity had no effect on the sorbent stabilized sulfidation capacity at 30 ppm H<sub>2</sub>S breakthrough. Thus, surface adsorption of H<sub>2</sub>S is a fast process. The corresponding regeneration off-gas distributions under the conditions of Figure 7 are shown in Table 5. We define the sorbent regenerability here as the ratio of total sulfur desorbed to total adsorbed sulfur, and this can be obtained by simply adding all desorbed sulfur amounts from the results listed in Table 5. It is clear that the regenerability was improved at higher sulfidation space velocity (SV = 80 000 h<sup>-1</sup>), for example, 95% vs 92% for CeO<sub>2</sub>, 90% vs 81% for Ce-70 at. % LaO<sub>x</sub>, and 98% vs 95% for 10 at. % Cu-CeO<sub>2</sub>. This corroborates our argument that a high space velocity suppresses bulk sorbent sulfidation. It also proves that the surface adsorption of H<sub>2</sub>S is very fast and limited only by the supply of gas to the surface. These results are important for practical design of the desulfurization/regeneration process using cerium oxide-based sorbents. Thus, high sulfidation space velocity offers the potential for compact sorber reactor design, while using a very high regeneration space velocity<sup>22,25</sup> will make the times required for sulfidation and regen-

(24) Akyurtlu, J. F.; Akyurtlu, A. *Chem. Eng. Sci.* **1999**, *54*, 2991–2997.

(25) Lowell, P. S.; Schwitzgebel, K.; Parsons, T. B.; Sladek, K. J. *Ind. Eng. Chem. Process Des. Dev.* **1971**, *10* (3), 384–390.

Table 5. Regeneration Off-Gas Composition

sorbent	temp (°C)	sulfidation space velocity <sup>a</sup> (h <sup>-1</sup> )	Regeneration, <sup>b</sup> 3% O <sub>2</sub> /He (%)		Reduction, <sup>c</sup> 50% H <sub>2</sub> -10% H <sub>2</sub> O/He (%)	
			(SO <sub>2</sub> ) <sub>out</sub> /(H <sub>2</sub> S) <sub>ads</sub>	(H <sub>2</sub> S) <sub>out</sub> /(H <sub>2</sub> S) <sub>ads</sub>	(SO <sub>2</sub> ) <sub>out</sub> /(H <sub>2</sub> S) <sub>ads</sub>	(H <sub>2</sub> S) <sub>out</sub> /(H <sub>2</sub> S) <sub>ads</sub>
CeO <sub>2</sub>	800	16 000	23.0	40.5	12.9	15.6
CeO <sub>2</sub>	800	80 000	14.3	52.3	5.7	22.8
Ce-70% LaO <sub>x</sub>	650	16 000	4.7	47.6	2.3	23.4
Ce-70% LaO <sub>x</sub>	800	16 000	7.3	47.8	2.4	23.5
Ce-70% LaO <sub>x</sub>	800	80 000	7.0	56.0	2.0	25.0
10% Cu-CeO <sub>2</sub>	650	16 000	25.8	24.9	15.1	23.1
10% Cu-CeO <sub>2</sub>	650	80 000	15.3	37.6	8.5	26.7
10% Cu-CeO <sub>2</sub>	800	16 000	14.4	56.6	2.9	21.1
10% Cu-CeO <sub>2</sub>	800	80 000	8.0	59.9	1.8	28.3

<sup>a</sup> Sulfidation: 650/800 °C, 0.1% H<sub>2</sub>S-50% H<sub>2</sub>-10% H<sub>2</sub>O-He, SV = 16 000 h<sup>-1</sup> or 80 000 h<sup>-1</sup>. <sup>b</sup> Regeneration: 650/800 °C, 3% O<sub>2</sub>-He, SV = 80 000 h<sup>-1</sup>. <sup>c</sup> Reduction: 650/800 °C, 50% H<sub>2</sub>-10% H<sub>2</sub>O-He, SV = 80 000 h<sup>-1</sup>.

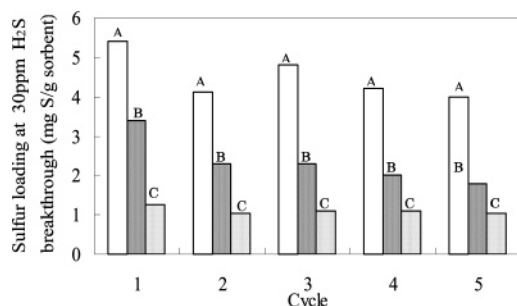


**Figure 6.** Sulfur capacity of 10% Cu-CeO<sub>2</sub> at 30 ppm H<sub>2</sub>S breakthrough in cyclic sulfidation/regeneration tests. Conditions for the results presented in panel A were as follows: prereduction: 650 °C, SV = 80 000 h<sup>-1</sup>; sulfidation: 650 °C, SV = 16 000 h<sup>-1</sup>; regeneration: 650 °C, SV = 80 000 h<sup>-1</sup>. Conditions for the results presented in panel B were as follows: prereduction: 650 °C, SV = 80 000 h<sup>-1</sup>; sulfidation: 650 °C, SV = 80 000 h<sup>-1</sup>; regeneration: 650 °C, SV = 80 000 h<sup>-1</sup>. Conditions for results presented in panel C were as follows: prereduction: 800 °C, SV = 80 000 h<sup>-1</sup>; sulfidation: 800 °C, SV = 16 000 h<sup>-1</sup>; regeneration: 800 °C, SV = 80 000 h<sup>-1</sup>. For all panels, the prereduction gas composition was 50% H<sub>2</sub>-10% H<sub>2</sub>O-He, the sulfidation gas composition is 0.1% H<sub>2</sub>S-50% H<sub>2</sub>-10% H<sub>2</sub>O-He, and the regeneration gas composition was 3% O<sub>2</sub>-He.

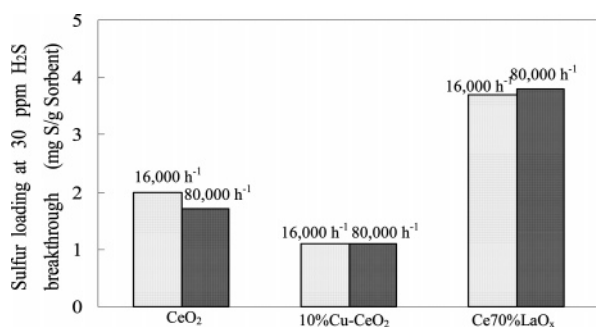


**Figure 7.** Stabilized sorbent sulfidation capacity at 30 ppm H<sub>2</sub>S breakthrough at two different sulfidation space velocities (SV = 16 000 and 80 000 h<sup>-1</sup>). Prereduction: 800 °C, 50% H<sub>2</sub>-10% H<sub>2</sub>O-He, SV = 80 000 h<sup>-1</sup>. Sulfidation: 800 °C, 0.1% H<sub>2</sub>S-50% H<sub>2</sub>-10% H<sub>2</sub>O-He. Regeneration: 800 °C, 3% O<sub>2</sub>-He, SV = 80 000 h<sup>-1</sup>.

eration more similar, so that only two reactors will be required, alternating as a sorber and a regenerator.<sup>22</sup>

To avoid sulfate formation during oxidative regeneration, potentially, other gas compositions<sup>22,26</sup> may be used at similarly high space velocities. This is the focus of a

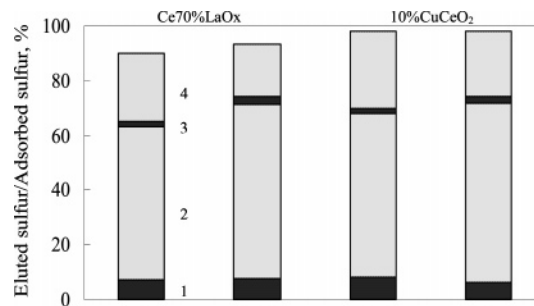


**Figure 8.** Stabilized regeneration off-gas composition at different regeneration space velocities: (A) SV = 80 000 h<sup>-1</sup> and (B) SV = 400 000 h<sup>-1</sup>. Prereduction: 800 °C, 50% H<sub>2</sub>-10% H<sub>2</sub>O-He, SV = 80 000 h<sup>-1</sup>. Sulfidation: 800 °C, 0.1% H<sub>2</sub>S-50% H<sub>2</sub>-10% H<sub>2</sub>O-He, SV = 80 000 h<sup>-1</sup>. Regeneration: 800 °C, 3% O<sub>2</sub>-He. Legend for figure: 1, percentage of SO<sub>2</sub> eluted in the 3% O<sub>2</sub>-He regeneration step; 2, percentage of H<sub>2</sub>S eluted in the 3% O<sub>2</sub>-He regeneration step; 3, percentage of SO<sub>2</sub> eluted in the 50% H<sub>2</sub>-10% H<sub>2</sub>O-He reduction step; and 4, percentage of H<sub>2</sub>S eluted in the 50% H<sub>2</sub>-10% H<sub>2</sub>O-He reduction step.

forthcoming paper.<sup>27</sup> It is also possible that a higher regeneration space velocity (SV > 80 000 h<sup>-1</sup>) can achieve this goal. As shown in Figure 8, for two sorbents, when the regeneration space velocity increased from SV = 80 000 h<sup>-1</sup> to SV = 400 000 h<sup>-1</sup>, the total desorbed sulfur amounts during the reduction step decreased from ~27% to ~22% and from ~30% to ~25% for Ce-70% LaO<sub>x</sub> and 10% Cu-CeO<sub>2</sub>, respectively. These results indicate that the sulfate formation during oxidative regeneration can be suppressed using higher regeneration space velocities, if the sulfidation was fully reversible and limited to the surface of the sorbent. The other advantage of using a higher regeneration space velocity here was that, without affecting the sulfur capacity and regenerability, the regeneration time was reduced 3-fold, approaching the time that was required for each surface sulfidation half-cycle.

## Conclusions

In this work, cerium oxide-based sorbents were evaluated for the regenerative removal of H<sub>2</sub>S from reformate-type gas mixtures at temperatures in the range of 650–800 °C. Copper- or lanthanum-containing cerium oxide materials with high surface areas were prepared

(26) Sakbodin, M. M.S. Thesis work, Tufts University, Medford, MA, in progress.

(27) Sakbodin, M.; Wang, Z.; Flytzani-Stephanopoulos, M. Unpublished work.



by the urea coprecipitation/gelation method, followed by slow heating and calcination in air at 650 °C for 4 h. Under both oxidative and reductive treatments at 800 °C, copper enhances the sintering of ceria, whereas lanthanum doping suppresses the crystal growth of ceria. However, the addition of copper improves the sulfidation kinetics of ceria, as demonstrated for the 10 at. % Cu–CeO<sub>2</sub> sorbent. Similarly low activation energies ( $15 \pm 2$  kJ/mol) for sulfidation were measured with all sorbent compositions, indicating that the reaction is adsorption-limited.

The regenerability of ceria-based sorbents and the regeneration off-gas composition can be controlled by proper choice of the operating conditions. The key parameters are temperature and sulfidation space velocity (SV). Thus, we have shown, in this work, for the first time, that it is possible to limit the sulfidation

reaction to the surface of the sorbent through the use of high space velocity ( $SV > 16\,000\text{ h}^{-1}$  at 800 °C). This surface adsorption is reversible, and thus the sulfided sorbents can be fully regenerated. Regeneration at high space velocities ( $SV > 80\,000\text{ h}^{-1}$ ) can be used to suppress sulfate formation and shorten the total time required for complete sorbent regeneration. This creates new opportunities for sorber/regenerator reactor design to meet the requirements of solid oxide fuel cell (SOFC) systems at any scale.

**Acknowledgment.** The financial support of this work by the Army Research Laboratory, Power and Energy Collaborative Technology Alliance is gratefully acknowledged.

EF049664A